Rapid Finite-Difference Computation of Subsonic and Slightly Supercritical Aerodynamic Flows

E. DALE MARTIN* AND HARVARD LOMAX†
NASA Ames Research Center, Moffett Field, Calif.

Rapid iterative (or semidirect) computation methods are developed for highly efficient finite-difference solution of the nonlinear equations of subsonic and transonic aerodynamics. Applicability is restricted to subsonic through slightly supercritical conditions. At each iteration, a fast, direct elliptic algorithm solves the entire computation field. A special acceleration device for the iterative convergence is developed. The methods are applied, using a recently developed direct Cauchy-Riemann solver, to the nonlinear transonic small-disturbance equations for a biconvex airfoil. At $M = 0.7$, $t/c = 0.1$ (subcritical), three iterations on a 39×32 mesh (totalling 2.45 sec on an IBM 360/67 computer) obtain convergence within 0.1%. A slightly supercritical case requires seven iterations (6.75 sec) for convergence within 1%. A very recent revision of the Cauchy-Riemann solver reduces these computing times by more than 30%. Strong supercritical cases do not converge, but the results, including the small computation times and the computational accuracy, demonstrate the usefulness of these techniques in subsonic flow computations through the critical condition and suggest the potential usefulness of further developments for transonic flow.

I. Introduction

CONTINUING development of more efficient computational techniques is needed, not only for increased economy in solving problems that can be treated by other methods, but also because such development can lead to successful solutions that would not otherwise be economically feasible with any available computer.

The purpose of the present investigation is to devise rapid iterative computation methods for the finite-difference solution of the nonlinear equations of steady, inviscid subsonic and transonic flows over airfoils. The approach is to use one of the fast, direct elliptic solvers[1-7] for each step within a rapidly converging iteration scheme. A combination of recent and present developments enables the direct solvers to be used efficiently in these nonlinear aerodynamic flow computations. The work reported here, which is restricted to subsonic and slightly supercritical flow, represents the first phase of this continuing investigation.

The methods currently receiving the most use in the numerical computation of steady subsonic and transonic irrotational flows about airfoils are the relaxation methods, such as the successively improved methods of Sells,[8] Murman and Cole,[9] Garabedian and Korn,[10] and Jameson.[11] Recently, Murman[12] made further improvements to the finite-difference algorithms in the relaxation approach.

The present approach is an alternative to the conventional relaxation methods and can be significantly faster, although handling of shock waves and geometry is not yet as highly developed. The direct solvers to be used at each iteration step are efficient because they take advantage of the highly ordered block structure of the matrix equations representing the finite-difference equations. When applied to certain forms of linear equations, these solvers are noniterative; they solve the entire computation field in a single closed sequence of steps, in contrast to iterative methods that do not have a predetermined number of operations. A semidirect method, i.e., an iteration scheme employing a direct solver at each step, is a "complete-block" iteration, as the ultimate addition to the sequence of "point-relaxation," "line-relaxation," and "block-relaxation" iterative methods. In the semidirect method, the complete block would cover the entire field of either a two- or three-dimensional problem.

The use of direct solvers within iteration schemes was recently considered by Roache[13] in treating the steady Navier-Stokes equations. Widlund[14] has briefly discussed similar procedures for general elliptic problems using devices such as Chebyshev acceleration and scaling to increase the convergence rate. Concus and Golub[15] have also investigated and further developed these iteration schemes to achieve rapid convergence in general elliptic problems.

Although fast, direct elliptic solvers have been used to some extent in fluid-dynamical problems with simple boundaries and simple boundary conditions (see Ref. 16 for examples), their use in more general problems, including aerodynamics, has been severely restricted because of the requirement of simple boundaries. The recent developments in Ref. 17 allow the efficient use of direct elliptic solvers in problems with arbitrary interior boundaries. Reference 18 included a calculation of inviscid subcritical compressible flow over a lifting airfoil using the full nonlinear equations for the stream function and using the technique of Ref. 17 to apply interior boundary conditions (on the airfoil) with a direct solver in an iteration scheme.

In this paper, we first consider a new approach to acceleration of iterative convergence using fast direct solvers. We then use this approach in a calculation of subsonic and slightly supercritical flow over a thin biconvex airfoil using the nonlinear transonic small-disturbance equations for the perturbation velocities and the Cauchy-Riemann solver presented in Ref. 7.

II. Rapid Numerical Iteration Techniques Using Direct Elliptic Solvers

Several different approaches to iteration using direct elliptic solvers are considered. For the various later applications, it is convenient to describe these approaches in some generality. (A specific simple example is given below for illustration.) Consider here a general system of nonlinear partial-differential equations in a domain R

$$\mathbf{LU} = \mathbf{F}\{\mathbf{U}, \mathbf{x}\} \quad \text{in} \quad R \tag{1}$$

where $\mathbf{U} = \mathbf{U}(\mathbf{x})$ is a vector function of the spatial position vector $\mathbf{x}$ and $\mathbf{L}$ is a linear elliptic differential operator chosen so that a discrete form of it can be handled by direct methods. The operator $\mathbf{L}$ can be the result of both scaling and shifting as discussed by Concus and Golub.[15] The notation, $\mathbf{F}\{\mathbf{U}, \mathbf{x}\}$ denotes that $\mathbf{F}$ may be a function of $\mathbf{x}, \mathbf{U}$, and the derivatives

Presented as Paper 74-11 at the AIAA 12th Aerospace Sciences Meeting, Washington, D.C., January 30–February 1, 1974; submitted July 1, 1974; revision received October 29, 1974.

Index category: Subsonic and Transonic Flow.

* Research Scientist, Computational Fluid Dynamics Branch. Associate Fellow AIAA.

† Chief, Computational Fluid Dynamics Branch. Member AIAA.

of $\mathbf{U}$ with respect to the components of $\mathbf{x}$. With this notation, nonseparable linear elliptic equations, nonlinear equations, or even mixed elliptic-hyperbolic equations can be represented formally. (An example of the latter is discussed in Sec. III.)

For the development following, it is also convenient to consider what we refer to as the extended form of Eq. (1):

$$\mathbf{LU} = (1-\varepsilon)\mathbf{F}\{\mathbf{U}_o, \mathbf{x}\} + \varepsilon\mathbf{F}\{\mathbf{U}, \mathbf{x}\} \quad \text{in} \quad R \tag{2}$$

where ε is an "artificial parameter" and $\mathbf{U}_o$ is some specified function of $\mathbf{x}$, such as an approximation to $\mathbf{U} = \mathbf{U}(\mathbf{x}, \varepsilon)$. Equation (2) is more general than Eq. (1), but the solution to Eq. (2) with special values of ε is useful for treating Eq. (1). For example, at $\varepsilon = 1$, the solution to Eq. (2) is the same as the solution to Eq. (1) with the same boundary conditions.

A. Method 1—Successive Approximations with Parameter

The simplest iteration scheme is the method of successive approximations. For this, Eq. (2) with $\varepsilon = 0$ gives an approximate form in which $\mathbf{U}_o$ may be interpreted as the result of a previous iteration and $\mathbf{U}$ is the next iterated result. In conventional relaxation methods, this form is usually combined with a "relaxation parameter," designated here as v. Such a scheme is commonly presented in two steps for iteration number $n = 1, 2, 3, \ldots$

$$\mathbf{L}\tilde{\mathbf{U}}_n = \mathbf{F}\{\mathbf{U}_{n-1}, \mathbf{x}\} \tag{3a}$$

where

$$\mathbf{U}_n = \mathbf{U}_{n-1} + v(\tilde{\mathbf{U}}_n - \mathbf{U}_{n-1}) \tag{3b}$$

If $v = 1$, this is the most straightforward method of successive approximations. Following the notation for conventional relaxation methods, the vector in parentheses in Eq. (3b) is called a "residual." Equations (3) are referred to as a preconverged form of Eq. (1).

B. Method 2—Series Expansion and Aitken/Shanks Formula

We introduce here a new approach to accelerating the iterative convergence based on one form of a set of transforms used by Aitken[19] and studied extensively by Shanks.[20] (According to Bellman,[21] the formula was first suggested by Kronecker.) The form of the Aitken/Shanks formula used here is

$$u^* = (u_1u_3 - u_2^2)/(u_1 - 2u_2 + u_3) \tag{4}$$

where $u^*(\mathbf{x})$ is an improved approximation to $u(\mathbf{x})$ resulting from the successive approximations $u_1(\mathbf{x})$, $u_2(\mathbf{x})$, and $u_3(\mathbf{x})$, and where u, u_1, u_2, and u_3 are each a component of the respective vectors $\mathbf{U}(\mathbf{x})$, $\mathbf{U}_1(\mathbf{x})$, $\mathbf{U}_2(\mathbf{x})$, and $\mathbf{U}_3(\mathbf{x})$. This formula is generally used to approximate a single quantity rather than a function $u(\mathbf{x})$ but here it is applied to each component u at each point in the field [$\mathbf{x}$ being a constant in Eq. (4)]. The formula is generally used to accelerate convergence of the iterates obtained in numerical computations by the conventional method of successive approximations.[22] During preparation of this paper, the authors learned of very recent work by Hafez and Cheng[23] in which they applied Eq. (4) to successive iterations of the velocity potential in a line-relaxation method for transonic-flow computations.

In many cases, the use of Eq. (4) with iterates obtained arbitrarily by successive approximations does not lead to a significantly improved approximation of $\mathbf{U}$. But a substantial and striking improvement can be gained if the successive iterates are obtained from truncated power series. The motivation for using power series rather than conventional successive approximations is the following. Shanks[20] has shown that the class of transforms of which Eq. (4) is a member works best if the sequence of approximations is nearly geometric. It is found, and is supported by examples, that the sequence of approximations is most nearly geometric if it is obtained from a power-series construction. The basis of the present approach is therefore the construction of successive numerical approximations by finite-difference solutions derived from formal power-series expansions to obtain as closely as possible a nearly geometric sequence for use in Eq. (4).

The motivation for proposing the extended form Eq. (2) is its convenience in constructing and determining formal power-series approximations for use in Eq. (4). Suppose the original problem to be solved consists of Eq. (1) along with appropriate boundary conditions, generally specified as

$$\mathbf{BU} = \mathbf{G}(\mathbf{x}) \quad \text{on} \quad C \tag{5}$$

where C is the boundary of the domain R of Eq. (1). Then consider the more general mathematical problem of Eq. (2) with condition Eq. (5) and the following facts: a) the solution to Eq. (2) with Eq. (5) generally depends on the specified $\mathbf{U}_o(\mathbf{x})$ as well as on ε; b) if $\varepsilon = 1$, the solution to Eq. (2) with Eq. (5) is also the solution to Eq. (1) with Eq. (5); c) if $\mathbf{U}_o(\mathbf{x}) = \mathbf{U}$, the solution to Eq. (2) with Eq. (5) is also the solution to Eq. (1) with Eq. (5); d) if $\mathbf{U}_o(\mathbf{x})$ can be used formally as an initial approximation to $\mathbf{U}$, then because of c, it is a good basis for formal successive approximations; and e) if $\mathbf{U}$ is expanded formally in powers of ε, substituted into the problem of Eq. (2) with Eq. (5), and the coefficients of powers of ε in the resulting equation are collected, then $\mathbf{U}_o$ can be treated precisely as an initial approximation and the resulting power-series solution in ε can be evaluated at $\varepsilon = 1$ to represent an approximate solution to Eq. (1).

The procedure is as follows. Formally expand $\mathbf{U}(\mathbf{x}, \varepsilon)$ in powers of ε

$$\mathbf{U}(\mathbf{x}, \varepsilon) \sim \mathbf{U}_1'(\mathbf{x}) + \varepsilon\mathbf{U}_2'(\mathbf{x}) + \varepsilon^2\mathbf{U}_3'(\mathbf{x}) + \cdots \tag{6}$$

[Although this is equivalent to a Taylor expansion about $\varepsilon = 0$, the subsequent use of the results in the Aitken/Shanks formula, Eq. (4), does not depend on the convergence of Eq. (6) at any specified value of ε (see Shanks[20]).] Substitute Eq. (6) into Eq. (2) and condition Eq. (5) and collect coefficients of powers of ε. This leads to the respective problems for $\mathbf{U}_1'$, $\mathbf{U}_2'$, and $\mathbf{U}_3'$:

$$\mathbf{LU}_1' = \mathbf{F}_o \text{ in } R \qquad \mathbf{BU}_1' = \mathbf{G}(\mathbf{x}) \text{ on } C \tag{7a}$$

$$\mathbf{LU}_2' = \mathbf{F}_1' - \mathbf{F}_o \text{ in } R \qquad \mathbf{BU}_2' = 0 \text{ on } C \tag{7b}$$

$$\mathbf{LU}_3' = \mathbf{F}_2' \text{ in } R \qquad \mathbf{BU}_3' = 0 \text{ on } C \tag{7c}$$

where

$$\mathbf{F}_o \equiv \mathbf{F}\{\mathbf{U}_o, \mathbf{x}\} \tag{8}$$

and where $\mathbf{F}\{\mathbf{U}, \mathbf{x}\}$ is expanded as

$$\mathbf{F}\{\mathbf{U}_1' + \varepsilon\mathbf{U}_2' + \cdots, \mathbf{x}\} = \mathbf{F}_1' + \varepsilon\mathbf{F}_2' + \cdots \tag{9}$$

Since the desired successive approximations $\mathbf{U}_1$, $\mathbf{U}_2$, $\mathbf{U}_3$, whose components are need for use in Eq. (4), are successive truncations of the series Eq. (6), we define the truncated series as

$$\begin{aligned} \mathbf{U}_1(\mathbf{x}) &= \mathbf{U}_1' & \mathbf{F}_1 &= \mathbf{F}_1' \\ \mathbf{U}_2(\mathbf{x}) &= \mathbf{U}_1' + \varepsilon\mathbf{U}_2' & \mathbf{F}_2 &= \mathbf{F}_1' + \varepsilon\mathbf{F}_2' \\ \mathbf{U}_3(\mathbf{x}) &= \mathbf{U}_1' + \varepsilon\mathbf{U}_2' + \varepsilon^2\mathbf{U}_3' \end{aligned} \tag{10}$$

Using Eqs. (10) in Eq. (7), we can then replace the problems, Eq. (7), by the respective problems for $\mathbf{U}_1$, $\mathbf{U}_2$, and $\mathbf{U}_3$. The final step is set $\varepsilon = 1$, with the results:

$$\mathbf{LU}_1 = \mathbf{F}_o \text{ in } R \qquad \mathbf{BU}_1 = \mathbf{G}(\mathbf{x}) \text{ on } C \tag{11a}$$

$$\mathbf{LU}_2 = \mathbf{F}_1 \text{ in } R \qquad \mathbf{BU}_2 = \mathbf{G}(\mathbf{x}) \text{ on } C \tag{11b}$$

$$\mathbf{LU}_3 = \mathbf{F}_2 \text{ in } R \qquad \mathbf{BU}_3 = \mathbf{G}(\mathbf{x}) \text{ on } C \tag{11c}$$

Since ε is 1, Eqs. (11) are problems for successive approximations to the solution of Eq. (1) with condition Eq. (5). Since the resulting $\mathbf{U}_1$, $\mathbf{U}_2$, and $\mathbf{U}_3$ at any $\mathbf{x}$ are the results of successive truncations of a formal power series, they are generally in a more nearly geometric sequence than would be the results of method 1, and so the components of each $\mathbf{U}_n$ are generally better for use in Eq. (4) to obtain an improved approximation.

Note that: a) If the right-hand side of Eq. (1) is linear in $\mathbf{U}(\mathbf{x})$, then the problems for the successive $\mathbf{U}_n$ in Eq. (11) will be equivalent to results from method 1, Eqs. (3), with $v = 1$; b) since $\mathbf{U}_o(\mathbf{x})$ in Eqs. (2) and (8) is arbitrary, it may be specified as zero, or as the result of a previous iteration. Thus, for example, one may specify $\mathbf{U}_o = 0$ for $n = 1$, find $\mathbf{U}_1$, $\mathbf{U}_2$, and $\mathbf{U}_3$, and use Eq. (4) to obtain an improved solution, which may then be used as the new $\mathbf{U}_o$ to start the sequence again; c) if $\mathbf{U}_o(\mathbf{x})$ is too close to the exact solution, then a large number of significant figures would

be needed for the quantities in Eq. (4). Without a large number of significant figures, both the numerator and denominator in Eq. (4) would be erroneous. Therefore, in numerical computations with limited significant figures, the use of Eq. (4) becomes inappropriate when $\mathbf{U}_o$ has been determined too closely to the correct solution at any point. As a result of this property, it has been found convenient to use method 2 for only one or two cycles to obtain an approximate solution close to the converged solution, then proceed to convergence using method 1 or other combinations of devices such as described by Concus and Golub.[15]

C. One-Dimensional Example

To illustrate very simply the application of methods 1 and 2 in an analytical example, consider the following simple one-dimensional problem: the nonlinear differential equation, with a linear operator, to be solved is

$$du/dx + u = (1/2)u^2 \quad \text{in} \quad 0 \leqq x < \infty \tag{12a}$$

with the boundary condition,

$$u(0) = 1 \tag{12b}$$

To solve Eqs. (12) by method 1 with $v = 1$, we put Eqs. (12) in the form of Eq. (3) for $n = 1, 2, 3, \ldots$

$$(d/dx + 1)u_n = (1/2)u_{n-1}^2 \tag{13a}$$

with

$$u_n(0) = 1 \tag{13b}$$

With the initial approximation $u_o(x) = 0$, the analytical results for $u_1(x)$, $u_2(x)$, and $u_3(x)$ evaluated at $x = 1$ are, respectively, $u_1(1) = 0.3678794412$, $u_2(1) = 0.4841515202$, and $u_3(1) = 0.5247721376$. If, in one approach, these successive approximations were put into formula (4) to obtain a better approximation, the result would be $u^*(1) = 0.546583145$, which is just slightly closer to the exact value, $u(1) = 0.5378828428$, than is the third approximation.

Consider now the solution to Eqs. (12) by method 2 as previously described. The extended form Eq. (2) of Eq. (12) is

$$du/dx + u = (1-\varepsilon)(1/2)u_o^2 + \varepsilon(1/2)u^2 \tag{14}$$

with condition (12b). Expanding $u(x)$ in powers of ε as in Eq. (6) and substituting it into Eq. (14) and Eq. (12b) lead to the problems corresponding to Eq. (7):

$$(d/dx + 1)u_1' = (1/2)u_o^2 \qquad u_1'(0) = 1 \tag{15a}$$

$$(d/dx + 1)u_2' = (1/2)[(u_1')^2 - u_o^2] \qquad u_2'(0) = 0 \tag{15b}$$

$$(d/dx + 1)u_3' = u_1'u_2' \qquad u_3'(0) = 0 \tag{15c}$$

or corresponding to Eqs. (11) with $\varepsilon = 1$ for the respective approximations $u_1(x)$, $u_2(x)$, and $u_3(x)$

$$(d/dx + 1)u_1 = (1/2)u_o^2 \qquad u_1(0) = 1 \tag{16a}$$

$$(d/dx + 1)u_2 = (1/2)u_1^2 \qquad u_2(0) = 1 \tag{16b}$$

$$(d/dx + 1)u_3 = (1/2)u_2^2 - (1/2)(u_1 - u_2)^2 \qquad u_3(0) = 1 \tag{16c}$$

Note that although Eqs. (16a) and (16b) are equivalent to Eqs. (13), there is a difference in Eq. (16c) because of the nonlinearity of the right side of Eq. (12a). With the initial approximation $u_o(x) = 0$, the analytical results evaluated at $x = 1$ are $u_1(1) = 0.3678794412$, $u_2(1) = 0.4841515202$, and $u_3(1) = 0.5209005060$. Now substituting these successive approximations, obtained from the power-series construction of method 2, into formula (4) yields the improved approximation, $u^*(1) = 0.537882842$. This result is the same to eight significant figures as the exact solution quoted above to 10 figures. The very high accuracy in this example occurs because the sequence found by method 2 is precisely geometric. Equation (4) then extrapolates to the exact solution. (The application in Sec. III below involves sequences that are not precisely geometric.) The previous example demonstrates the power of method 2, in contrast to method 1, in obtaining successive approximations that are most appropriate for use in the Aitken/Shanks formula for accelerating iterative convergence.

D. Specific Forms of LU = F

In Ref. 18 and Sec. III below, the specific forms of Eq. (1) treated numerically using fast, direct elliptic solvers are

$$\nabla^2\psi = F\{\psi\} \tag{17}$$

and

$$\begin{bmatrix} \partial/\partial x & \partial/\partial y \\ \partial/\partial y & -\partial/\partial x \end{bmatrix} \begin{bmatrix} u \\ v \end{bmatrix} = \begin{bmatrix} s\{u\} \\ 0 \end{bmatrix} \tag{18}$$

The continuous forms of the iteration procedures were previously described. The discretized forms depend on the particular forms of Eqs. (17) and (18) and are discussed later. Although the operator matrix on the left-hand side of Eq. (18) is purely elliptic, the discretized forms in Sec. III can also handle embedded hyperbolic regions by modifying the right-hand side of Eq. (18) (to be shown).

E. Iterative Convergence

An excellent discussion of the convergence of semidirect methods applied to nonseparable linear elliptic equations is given by Concus and Golub.[15] It is instructive to apply such an analysis to method 1 applied to a linear elliptic form of Eq. (17), and this has been done in Ref. 18, where the optimum relaxation parameter v and the corresponding convergence rate are determined.

III. Solution to Transonic Small-Disturbance Equations for a Biconvex Airfoil

Consider now the solution to the nonlinear small-disturbance equations for steady, irrotational, subsonic or transonic flow of a perfect gas over a thin symmetrical parabolic-arc biconvex airfoil alined with a uniform subsonic free stream. Steger and Lomax[24] have shown that the first-order system of partial-differential equations in terms of the "primitive variables" (velocity components and density) could be used successfully in a generalized relaxation procedure for transonic airfoil flow computations. It is found here that the finite-difference operators for the small-disturbance velocity potential of transonic flow in the relaxation method of Murman and Cole,[9] as recently improved by Murman,[12] adapt most naturally to the small-disturbance, first-order partial-differential equations for the perturbation velocity components. Our colleague, Dr. E. Murman, has independently come to the same conclusion. In the present treatment, the semidirect methods 1 and 2 of Sec. II are used to solve these equations in the discretized basic form of Eq. (18), with a direct Cauchy-Riemann solver[7] used for the elliptic operator. The advantages of a certain scaling of the equations for the semidirect methods, as well as the advantages of the appropriate use of the Aitken/Shanks formula in method 2 over the straightforward method 1, are investigated. A slightly supercritical (mixed elliptic-hyperbolic) case is described in the Results, as well as subcritical examples.

A. Small-Disturbance Equations for Thin Airfoil

Let the x-axis be in the direction of the airfoil chord and the y-axis be normal to the chord and bisect it. Both x and y are normalized by the chord length c. Let U and V be the x and y components of velocity normalized by the freestream velocity q_∞, M_∞ be the freestream Mach number, and γ be the ratio of specific heats. The approximate relations for the dimensionless perturbation velocities u and v are taken to be

$$U = 1 + \tau u \qquad V = \tau v \tag{19}$$

where τ is the small thickness ratio of the airfoil. The transonic small-disturbance equations are then

$$u_x + v_y = bu_x + a(u^2)_x \tag{20a}$$

$$u_y - v_x = 0 \tag{20b}$$

where

$$b = M_\infty^2 \qquad a = (1/2)(\gamma + 1)M_\infty^2\tau \tag{21}$$

The corresponding pressure coefficient is $C_p = -2\tau u$. For the nonlifting case considered here, the exterior conditions are $u, v \to 0$ as $x^2 + y^2 \to \infty$, and the thin-airfoil condition representing flow tangency at the surface is that $\tau v(x, 0)$ equal the airfoil slope at the corresponding x.

A convenient scaling of the preceding problem is accomplished by the Prandtl-Glauert transformation, using $\beta \equiv (1 - M_\infty{}^2)^{1/2}$; thus

$$u(x, y) = (1/\beta)\bar{u}(x, \bar{y}) \tag{22a}$$

$$v(x, y) = \bar{v}(x, \bar{y}) \tag{22b}$$

$$y = (1/\beta)\bar{y} \tag{22c}$$

transforms the small-disturbance equations to

$$\bar{u}_x + \bar{v}_{\bar{y}} = \bar{a}(\bar{u}^2)_x \tag{23a}$$

$$\bar{u}_{\bar{y}} - \bar{v}_x = 0 \tag{23b}$$

where

$$\bar{a} = a/\beta^3 = (1/2)(\gamma + 1)M_\infty{}^2\tau(1 - M_\infty{}^2)^{-3/2} \tag{23c}$$

and the corresponding pressure coefficient is $C_p = -2(\tau/\beta)\bar{u}$. For the biconvex airfoil, the boundary conditions are

$$\bar{v}(x, 0) = -4x \quad (-0.5 < x < 0.5) \tag{23d}$$

$$= 0 \quad (|x| > 0.5) \tag{23e}$$

$$\bar{u}, \bar{v} \to 0 \quad \text{as} \quad x^2 + \bar{y}^2 \to \infty \tag{23f}$$

Note that a) the solution depends on a single similarity parameter $\bar{a}$, like the usual transonic similarity parameters[25,26] K or K_1; b) the linearized Prandtl-Glauert approximation is obtained by simply setting $\gamma = -1$, leaving $\bar{a} = 0$; and c) the condition at infinity when $\bar{a} \neq 0$ can be replaced conveniently by the approximate condition of the analytical Prandtl-Glauert solution applied on a finite boundary at some distance from the airfoil; in terms of the complex variable $z = x + i\bar{y}$, it is

$$(\bar{u} - i\bar{v})_{PG} = \frac{4}{\pi}\left[1 - z \log\left(\frac{z + 0.5}{z - 0.5}\right)\right] \tag{24}$$

One drawback of the formulation, Eq. (23), is that it cannot be used at $M_\infty = 1$.

Both series of Eqs. (20) and (23) may be put into the form

$$(1 - b - 2au)u_x + v_y = 0 \tag{25a}$$

$$u_y - v_x = 0 \tag{25b}$$

where the variables and parameters are understood to have "bars" if Eqs. (23) are being considered, and where $\bar{b} = 0$. Equations (25) change type where the coefficient of u_x changes sign. This defines the critical velocity:

$$u_{CR} = (1 - b)/2a \qquad \bar{u}_{CR} = 1/2\bar{a} \tag{26}$$

(Note that $1/2\bar{a} = (-K_1)^{3/2}$, where K_1 is the similarity parameter on page 237 of Ref. 26.) The corresponding critical pressure coefficient is $C_p{}^* = -2\tau u_{CR} = -2(\tau/\beta)\bar{u}_{CR}$. Equations (25) are elliptic, parabolic, or hyperbolic, depending on whether $u < u_{CR}$, $u = u_{CR}$, or $u > u_{CR}$. For numerical computations, we apply finite-differencing schemes only to the conservation form of the transonic Eqs. (20) or (23). Equations (25) are used only to determine the choice of difference operator, as described in Sec. IIIB.

B. Converged Forms of Difference Equations

Murman[12] discusses four different types of finite-difference operators: elliptic, hyperbolic, parabolic, and shock-point. The first two apply at points where the chosen difference equations are clearly elliptic or hyperbolic and the last two apply near where the flow is in the process of changing from one to another. The difference formulas described here (in the converged form) are identical to Murman's except that they are in terms of u and v rather than the velocity potential.

The adaptation of type-dependent difference operators for the velocity potential to the velocity components is straightforward if a staggered u, v mesh is used. The Cauchy-Riemann solver[7] employs a staggered mesh for u and v that is particularly suited for use with difference operators equivalent to Murman's. Figure 1

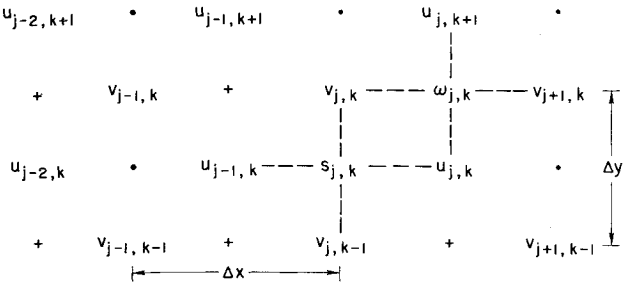

Fig. 1 Staggered meshes for u and v.

shows the pattern of u and v points (indexed by j in the x direction and k in the y direction) that is used in Ref. 7 and that also will be used here. The dots and "s points" in Fig. 1 are points at which the "continuity equation," Eqs. (20a), (23a), or (25a), is to be satisfied. The crosses, or "ω points" are points at which the "vorticity equation," Eqs. (20b) or (23b), is to be satisfied.

First consider the vorticity equation. For all j, k, regardless of whether the point $\omega_{j,k}$ in Fig. 1 is in an elliptic or a hyperbolic region, both derivatives in this equation are replaced by central differences because nothing about this equation changes when the system changes type. Maintaining central differencing everywhere simply guarantees conservation of both local and global vorticity. If we denote a central difference for a derivative by subscript c, the general finite-difference representation of the vorticity equation is simply

$$u_{yc} - v_{xc} = 0 \tag{27}$$

Next consider the continuity equation. The differencing schemes applied to this equation change as the system changes type. The type depends on the sign of $u - u_{CR}$. [In the following discussion, the variables and parameters are understood to have "bars" if Eqs. (23) are being considered.] It is convenient to define certain "test variables," which we denote as $(u_e)_{j,k}$ and $(u_h)_{j,k}$, corresponding to each point $s_{j,k}$. The precise definitions will depend on the specific differencing schemes chosen, but $(u_e)_{j,k} < u_{CR}$ means the chosen elliptic difference operator is appropriate at point $s_{j,k}$, and $(u_h)_{j,k} > u_{CR}$ means the chosen hyperbolic difference operator is appropriate. Following Murman,[12] we define the four different types of points in the transonic field as in Table 1.

The operators at points designated H and S include upstream or "backward differences." In the following, a backward-difference form of a derivative is denoted by subscript b.

Since the direct Cauchy-Riemann solver to be used always solves an elliptic operator that is central differenced, it is convenient to write the difference form of the continuity equation in the following way. At any $s_{j,k}$ point,

$$u_{xc} + v_{yc} = s_{j,k}\{u\} \tag{28}$$

where

$$E: \quad s_{j,k}\{u\} = bu_{xc} + a(u^2)_{xc} \tag{29a}$$

$$H: \quad s_{j,k}\{u\} = (b - 1)u_{xb} + u_{xc} + a(u^2)_{xb} \tag{29b}$$

$$P: \quad s_{j,k}\{u\} = u_{xc} \tag{29c}$$

$$S: \quad s_{j,k}\{u\} = (b - 1)u_{xb} + bu_{xc} + a[(u^2)_{xc} + (u^2)_{xb}] \tag{29d}$$

Even though the difference Eqs. (28) and (27) have an elliptic operator on the left, their actual type after convergence depends

Table 1 Types of points in the transonic field

Test	Type of point $s_{j,k}$
Both $(u_h)_{j,k}$ and $(u_e)_{j,k} < u_{CR}$:	Elliptic (E)
Both $(u_h)_{j,k}$ and $(u_e)_{j,k} > u_{CR}$:	Hyperbolic (H)
$(u_h)_{j,k} < u_{CR} < (u_e)_{j,k}$:	Parabolic (P)
$(u_e)_{j,k} < u_{CR} < (u_h)_{j,k}$:	Shock (S)

on u_e and u_h relative to u_{CR}. Because of this, we refer to them as the general finite-difference converged form of the transonic equations.

The general difference Eqs. (27) and (28) are now made specific according to the form of the differencing used in the Cauchy-Riemann solver.[7] From Fig. 1, we see that central differences about the point $s_{j,k}$ are

$$u_{xc} = (u_{j,k} - u_{j-1,k})/\Delta x \tag{30a}$$

$$v_{yc} = (v_{j,k} - v_{j,k-1})/\Delta y \tag{30b}$$

The form for $(u^2)_x$ is, of course, the same as for u_x. These are second-order accurate. A backward difference referred to the point designated $s_{j,k}$ may be selected as

$$u_{xb} = (u_{j-1,k} - u_{j-2,k})/\Delta x \tag{31}$$

which is first-order accurate for use in hyperbolic regions. (Other forms of backward differencing could be used since these quantities appear only in the right side of Eqs. (29).) The corresponding central differences for Eq. (27), about the point designated by $\omega_{j,k}$ in Fig. 1, are

$$u_{yc} = (u_{j,k+1} - u_{j,k})/\Delta y \tag{32a}$$

$$v_{xc} = (v_{j+1,k} - v_{j,k})/\Delta x \tag{32b}$$

Direct substitution of Eqs. (31–33) into Eqs. (27) and (28) provides the converged form of the finite-difference equations to be solved.

It remains to determine the appropriate test velocities $(u_e)_{j,k}$ and $(u_h)_{j,k}$. Following Murman's approach,[12] we put the purely elliptic and hyperbolic forms of Eq. (28) with Eqs. (29a) or (29b) and with Eqs. (30) and (31) into the form suggested by Eqs. (25) to determine the conditions for the difference equations to be valid. If we let $\mu = \Delta y/\Delta x$, then Eq. (24) for an "E point" becomes

$$[\mu(1-b) - \mu a(u_{j,k} + u_{j-1,k})](u_{j,k} - u_{j-1,k}) + (v_{j,k} - v_{j,k-1}) = 0 \tag{33}$$

The bracketed coefficient is positive if

$$(u_e)_{j,k} \equiv (1/2)(u_{j,k} + u_{j-1,k}) < (1-b)/2a = u_{CR} \tag{34}$$

Similarly, Eq. (28) for an "H point" becomes

$$[\mu(1-b) - \mu a(u_{j-1,k} + u_{j-2,k})](u_{j-1,k} - u_{j-2,k}) + (v_{j,k} - v_{j,k-1}) = 0 \tag{35}$$

The bracketed coefficient is negative if

$$(u_h)_{j,k} \equiv (1/2)(u_{j-1,k} + u_{j-2,k}) > (1-b)/2a = u_{CR} \tag{36}$$

We note that, with the differences Eqs. (30–32),

$$(u_h)_{j,k} = (u_e)_{j-1,k}$$

C. Preconverged Forms of Difference Equations

On the basis of the previous so-called converged forms of the difference equations, which are essentially equivalent to Murman's difference equations for the velocity potential, we now consider the corresponding preconverged forms applicable to the semidirect methods 1 and 2 discussed in Sec. II.

Application of the procedure for method I in Sec. II to the previous equations leaves the following preconverged form [cf. Eqs. (3)]:

$$(\tilde{u}_{xc} + v_{yc})_n = s_{j,k}\{u_{n-1}\} \tag{37a}$$

$$(\tilde{u}_{yc} - v_{xc})_n = 0 \tag{37b}$$

where

$$u_n = u_{n-1} + \nu(\tilde{u}_n - u_{n-1}) \tag{37c}$$

in which $s_{j,k}\{u_{n-1}\}$ is given by Eqs. (29). The direct Cauchy-Riemann solver can be applied at each n to solve these difference equations.

For method 2 in Sec. II, the difference Eqs. (28) and (27) are written initially in the extended form [cf. Eq. (2)]:

$$u_{xc} + v_{yc} = (1-\varepsilon)s_{j,k}\{u_o\} + \varepsilon s_{j,k}\{u\} \tag{38a}$$

$$u_{yc} - v_{xc} = 0 \tag{38b}$$

If both $u(x, y, \varepsilon)$ and $v(x, y, \varepsilon)$ are expanded in powers of ε [Eq. (6)], the resulting finite-difference problems for the successive approximations u_1, u_2, u_3, and v_1, v_2, v_3, which are successive truncations of the power series for $n = 1, 2, 3$, are given by [cf. Eqs. (11)]:

$$(u_n)_{xc} + (v_n)_{yc} = s_{n-1} \tag{39a}$$

$$(u_n)_{yc} - (v_n)_{xc} = 0 \tag{39b}$$

with discrete forms of the conditions:

$$\begin{aligned} &\text{on} \quad x = x_l \quad \text{and} \quad y = y_u: \quad u_n = u_{PG} \\ &\text{on} \quad x = x_r: \quad v_n = v_{PG} \\ &\text{on} \quad y = 0: \quad v_n = -4x \ (-0.5 < x < 0.5) \\ &\qquad\qquad = 0 \ (|x| > 0.5) \end{aligned} \tag{40}$$

The s_{n-1} terms in Eq. (39a) are obtained by substituting the ε power series for u into Eqs. (29) for use in (38a). The resulting truncations are, for $n = 1$ and 2 in Eq. (39a):

$$\begin{aligned} &E: \quad s_{n-1} = [bu_{xc} + a(u^2)_{xc}]_{n-1} \\ &H: \quad s_{n-1} = [(b-1)u_{xb} + u_{xc} + a(u^2)_{xb}]_{n-1} \\ &P: \quad s_{n-1} = [u_{xc}]_{n-1} \\ &S: \quad s_{n-1} = [(b-1)u_{xb} + bu_{xc}]_{n-1} + a[(u^2)_{xc} + (u^2)_{xb}]_{n-1} \end{aligned} \tag{41}$$

$n = 3$ in Eq. (39a):

$$\begin{aligned} &E: \quad s_2 = b(u_2)_{xc} + a[{u_2}^2 - (u_2 - u_1)^2]_{xc} \\ &H: \quad s_2 = (b-1)(u_2)_{xb} + (u_2)_{xc} + a[{u_2}^2 - (u_2 - u_1)^2]_{xb} \\ &P: \quad s_2 = (u_2)_{xc} \\ &S: \quad s_2 = (b-1)(u_2)_{xb} + b(u_2)_{xc} + a[{u_2}^2 - (u_2 - u_1)^2]_{xb} + \\ &\qquad a[{u_2}^2 - (u_2 - u_1)^2]_{xc} \end{aligned} \tag{42}$$

Substituting Eqs. (30–32) into Eqs. (39–42) yields the final forms of the difference equations to be solved by the Cauchy-Riemann solver for $n = 1, 2, 3$. The resulting values of u_n at each j, k are then put into the Aitken/Shanks formula Eq. (4) for an improved approximation. As discussed in Sec. II, the resulting $u^*_{j,k}$ may then be used as the new u_o to repeat the procedure for another three successive approximations; or the procedure can then be switched to method 1 if the numerator or denominator of Eq. (4) should become too small at any j, k so that an erroneous u^* would be produced by lack of significant figures.

D. Computational Considerations

In considering whether to use method 2, one must account for the fact that a total of four arrays with the dimensions of $u_{j,k}$ and $v_{j,k}$ is needed. The two additional arrays are needed to store u_1 and u_2 while $u = u_3$ is being determined. Then $u_{j,k}$ is replaced by the results of the Aitken/Shanks formula; the $u_{j,k}$ array is then used to obtain $s_{j,k}$ which is put into $v_{j,k}$ to start the next iteration in using the Cauchy-Riemann solver.[7] In contrast, method 1 with $\nu = 1$ requires only $u_{j,k}$ and $v_{j,k}$ since $s_{j,k}$, formed from the previous iteration for $u_{j,k}$, is put into $v_{j,k}$ to start the next iteration in using the Cauchy-Riemann solver. If $\nu \neq 1$, then an additional array u_1 is needed.

E. Results for Biconvex Airfoil

The previous procedures for both methods 1 and 2 were applied to a parabolic-arc biconvex airfoil. In the cases computed, the Prandtl-Glauert analytical solution was applied as the exterior condition on boundaries at $x = -1$ and (about) $x = +1$, and on the upper boundary at $\bar{y} = \beta y = 2.0$. For most cases computed, the number of points at which each equation was satisfied was $NX = 39$ in the x direction (so that $\Delta x = 0.05$) and $NY = 32$ in the y direction (so that $\Delta \bar{y} = 0.0625$). The discretized conditions on v at $y = 0$ straddled the leading and trailing edges ($x = \mp 0.5$) so that u and C_p were computed there, and for $NX = 39$ those conditions were applied at 20 points along the airfoil chord.

The special case $\gamma = -1$ (for which the exact solution is the Prandtl-Glauert solution) has provided an effective illustration of the advantages of method 2 over method 1. Reference 18 gives details of comparisons of the iterative convergence.

A subcritical pressure distribution for $\gamma = 1.4$, at $M_\infty = 0.7$, $\tau = 0.10$ (for which $C_p{}^* = -0.8673$) is shown plotted in Fig. 2. For comparison are shown the analytical Prandtl-Glauert linearized-theory results and results of numerical computations

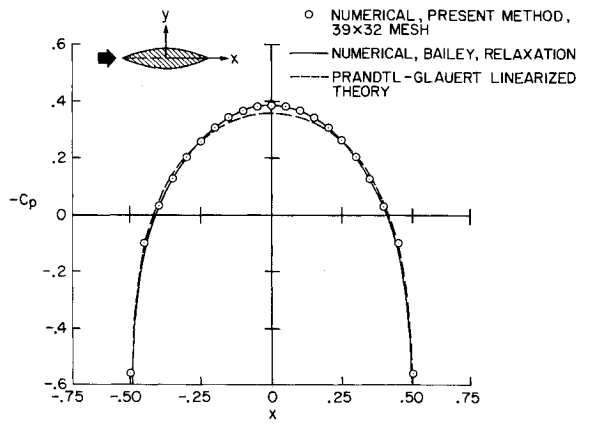

Fig. 2 Pressure on 10% thick biconvex airfoil at $M = 0.7$, $\gamma = 1.4$ (subcritical).

supplied by our colleague, F. R. Bailey. Bailey's program solves the transonic small-disturbance equation for the velocity potential using the difference operators of Murman.[12] His results were computed with $\Delta x = 0.02$ on the airfoil and with upstream and downstream boundaries at $x = \mp 2.68$ and the upper boundary at $y = 7.105$. The present results for the 39×32 mesh with boundaries as previously described ($\Delta x = 0.05$) agree well with those of Bailey.

The iterative convergence for the subcritical case in Fig. 2 is illustrated in Fig. 3 along with results for convergence at other subcritical conditions. The percent error in the peak pressure (at or near the center) from its converged value is used as a convenient indicator of the degree of convergence (although the "maximum residual" test parameter is used in the computer program). Figure 3 shows the number of iterations n and the corresponding computing time on the IBM 360/67 vs M_∞ for the *P-G* scaled Eqs. (23). Results for method 1 are shown by open symbols and, for method 2, by solid symbols. All these computations started with the initial condition $u_0(x, y) = 0$. For the example case of Fig. 2 ($M_\infty = 0.7$) the solid-triangle symbol on Fig. 3 shows that the peak pressure is obtained with less than 0.1% error in three iterations and application of the Aitken/Shanks formula (2.45 sec on the IBM 360/67 computer).

A slightly supercritical pressure distribution (at $M_\infty = 0.8$, $\tau = 0.10$, $\gamma = 1.4$, for which $C_p{}^* = -0.46875$) is shown plotted in Fig. 4. Present results are again compared with those obtained from Bailey's relaxation program. For this case, his upper boundary was at $y = 6.5$, the boundaries for present calculations being those specified earlier. The present results for the 39×32 mesh are shown by solid circles in Fig. 4. For this case, there was only one row of points for the u-mesh (Fig. 1), at $\bar{y} = 0.03125$,

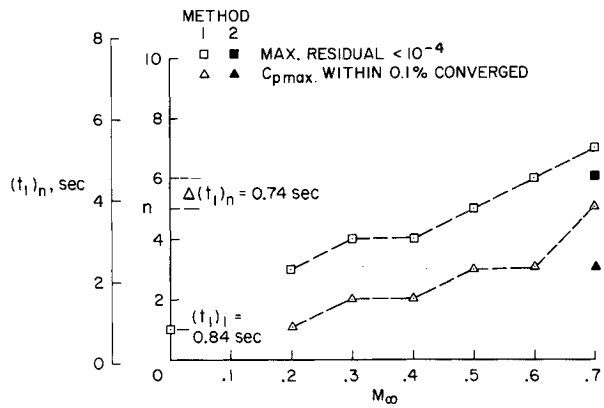

Fig. 3 Iterations for convergence in subcritical flow over biconvex airfoil (10% thickness, $\gamma = 1.4$, *P-G* scaled, 39×32 mesh; $(t_2)_n = (t_1)_n + 0.13$ sec, where $(t_2)_n$ and $(t_1)_n$ are total computing times for n iterations in methods 2 and 1 measured on IBM 360/67 using FORTRAN IV, level H, OPT = 2 compiler).

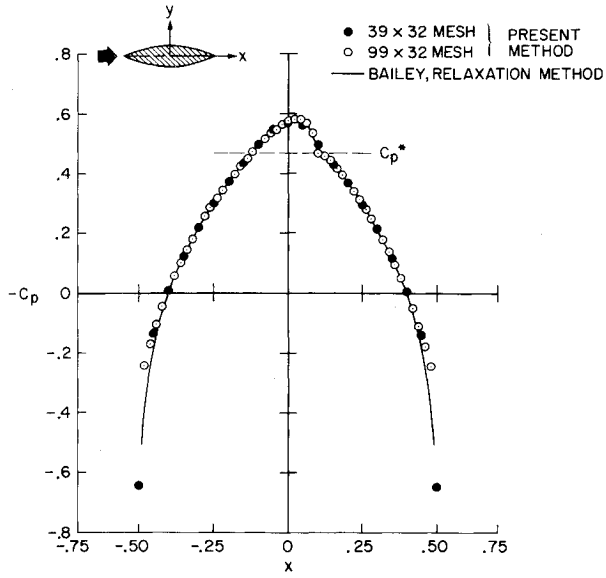

Fig. 4 Pressure on 10% thick biconvex airfoil at $M_\infty = 0.8$, $\gamma = 1.4$ (slightly supercritical).

inside the supersonic region, and on this row there were five nonelliptic points designated $s_{j,k}$ (one P, three H, and one S) where Eq. (37a) or (39a) was solved. In spite of this coarse mesh, the results shown in Fig. 4 are reasonably accurate. (Although the conservative shock-point operator of Murman[12] was used in both calculations, $C_p{}^*$ is not at the middle of the jump because of the weakness of the shock and coarseness of the mesh at the aft boundary of the small supersonic bubble, where the logarithmic singularity is not resolved.) The corresponding sonic points, found by linear interpolation of velocities, are shown as solid circles in Fig. 5.

To check the capability of the method with a finer mesh, $NX = 99$ was specified, with $\Delta x = 0.02$ on the body (and the same NY as before). The results are shown in Fig. 4 by the open circles. Except right at the peak and the shock, the results are the same as for $NX = 39$, but at the peak and shock they agree more closely with Bailey's computation.

Because only one row of u-mesh points is inside the hyperbolic region for $NY = 32$ ($\Delta\bar{y} = 0.0625$), a case was run with $NX = 39$ and $NY = 128$, which put five rows of u-mesh points (and s points) inside the hyperbolic region. The results on $y = 0$ were essentially identical to those for the 39×32 mesh in Fig. 4; the additional sonic points found by linear interpolation are shown in Fig. 5. The sonic points from the coarse 39×32 mesh calculation are well in line with those from the 39×128 mesh calculation. The aft sonic point (i.e., the shock) obtained at $y = 0$ by linear interpolation in the 99×32 mesh calculation is moved a significant distance forward of those from the calculations for $NX = 39$, indicating a more nearly normal shock wave.

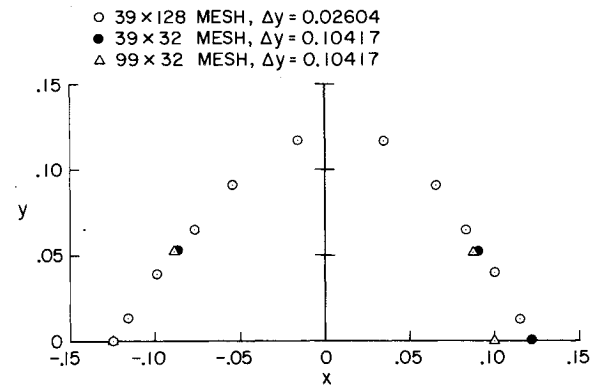

Fig. 5 Sonic line over 10% thick biconvex airfoil at $M_\infty = 0.8$, $\gamma = 1.4$ by linear interpolations.

F. On the Iterative Convergence of the Slightly Supercritical Computation

Whereas a programmed method without the type-dependent operators, using central differences everywhere [i. e., Eq. (29a)], became unstable (i.e., did not converge) for the slightly supercritical case $M_\infty = 0.8$, $\tau = 0.1$, the type-dependent methods previously outlined definitely converged for this slightly supercritical condition. The validity and stability of the iteration for this case were confirmed: by using different mesh spacings with essentially the same results; by using the 39×128 mesh which included a significant number (20) of nonelliptic points in five rows; by using a 99×32 mesh ($\Delta x = 0.02$) to resolve the shock wave; by running the program long to insure complete convergence (maximum normalized residual $< 5 \times 10^{-6}$ at all points); and by comparing the final results with computations by Bailey's program using Murman's[12] line-relaxation method.

The iterative convergence of the various methods applied to the *P-G* scaled equations for the slightly supercritical case on the 39×32 mesh is shown in Table 2. Whereas method 1 had converged to within 1% in 12 iterations (11.20 sec on the IBM 360/67 computer), method 2 with two successive applications of the Aitken/Shanks formula (six iterations) followed by switching to method 1 with $\nu = 1.2$, converged to the same accuracy in only seven iterations (6.75 sec) and to within 0.1% in 14 iterations (13.37 sec). Each of these computations started with $u_0(x, y) = 0$. (A very recently revised version of the Cauchy-Riemann solver that was presented in Ref. 7 achieves a more than 30% reduction in the computing times quoted in this paper.)

At the stage of development of the methods as described above, the cases that were tried for stronger supercritical conditions had not obtained complete convergence. There are, however, more recent indications from work now in progress that modifications in the second phase of this investigation will allow the methods to be extended to higher Mach numbers. There appears to be no fundamental reason why there should not be developed a degree of success in obtaining converged solutions similar to that obtained in using line-relaxation methods for higher supercritical Mach numbers.

IV. Conclusions

As an alternative to the conventional relaxation methods in use, new semidirect methods have been proposed and are in a state of continuing development. These use fast, direct numerical elliptic solvers within iteration schemes for computing solutions to nonlinear flow problems. Considered to be the main contribution here is a scheme that determines appropriate successive approximations for use in the Aitken/Shanks formula to accelerate the iterative convergence in these methods.

The application of the method in this paper includes the first use of the Cauchy-Riemann solver within an iterative scheme for solving a first-order system of nonlinear equations. In both subcritical and slightly supercritical inviscid flows over a biconvex airfoil, the leading-edge and trailing-edge singularities introduce no convergence difficulties and are captured with ease at each step. The numerical results in both cases agree well with other similar computations using a line-relaxation method. It is significant that the method has been shown to have some success, with rapid convergence, in a slightly supercritical flow, i.e., in a problem with mixed elliptic and hyperbolic regions. Further developments and improvements of these methods are in progress.

The rapid convergence achieved in the iterations using direct solvers in nonlinear problems, the consequent very small computation times, and the accuracy of the computed results demonstrate the usefulness of these techniques in subsonic flow computations through the critical condition and suggest the potential usefulness of further developments for transonic flow computations.

Table 2 Iterations for convergence of peak pressure on a 10% thick biconvex airfoil at $M_\infty = 0.8$, $\gamma = 1.4$ (slightly supercritical) on 39×32 mesh[a]

Method	$C_{p_{max}}$ within 1% converged		$C_{p_{max}}$ within 0.1% converged	
	n	t_n, sec	n	t_n, sec
Method 1	12	11.20	20	18.56
Method 2, $n = 1$ to 3, then method 1, $\nu = 1.0$	11	10.50	18	17.15
Method 2, $n = 1$ to 6, then method 1, $\nu = 1.0$	7	6.75	17	16.38
Method 2, $n = 1$ to 6, then method 1, $\nu = 1.2$	7	6.75	14	13.37

[a] t_n is the total computing time for n iterations using IBM 360/67 computer, FORTRAN IV, level *H*, OPT = 2 compiler.

References

[1] Buneman, O., "A Compact Non-Iterative Poisson Solver," SUIPR Rept. 294, May 1969, Institute for Plasma Research, Stanford University, Stanford, Calif.

[2] Hockney, R. W., "A Fast Direct Solution of Poisson's Equation Using Fourier Analysis," *Journal of the Association for Computing Machinery*, Vol. 12, Jan. 1965, pp. 95–113.

[3] Hockney, R. W., "The Potential Calculation and Some Applications," in *Methods in Computational Physics*, Vol. 9, edited by B. Alder, S. Fernbach, and M. Rotenberg, Academic Press, New York, 1970, pp. 135–211.

[4] Dorr, F. W., "The Direct Solution of the Discrete Poisson Equation on a Rectangle," *SIAM Review*, Vol. 12, Apr. 1970, pp. 248–263.

[5] Buzbee, B. L., Golub, G. H., and Nielson, C. W., "On Direct Methods for Solving Poisson's Equations," *SIAM Journal on Numerical Analysis*, Vol. 7, Dec. 1970, pp. 627–656.

[6] Le Bail, R. C., "Use of Fast Fourier Transforms for Solving Partial Differential Equations in Physics," *Journal of Computational Physics*, Vol. 9, June 1972, pp. 440–465.

[7] Lomax, H. and Martin, E. D., "Fast Direct Numerical Solution of the Nonhomogeneous Cauchy-Riemann Equations," *Journal of Computational Physics*, Vol. 15, May 1974, pp. 55–80.

[8] Sells, C. C. L., "Plane Subcritical Flow Past a Lifting Airfoil," *Proceedings of the Royal Society (London)*, Vol. A308, 1968, pp. 377–401.

[9] Murman, E. M. and Cole, J. D., "Calculation of Plane Transonic Flows," *AIAA Journal*, Vol. 9, Jan. 1971, pp. 114–121.

[10] Garabedian, P. R. and Korn, D. G., "Analysis of Transonic Airfoils," *Communications on Pure and Applied Mathematics*, Vol. XXIV, 1971, pp. 841–851.

[11] Jameson, A., "Transonic Flow Calculations for Airfoils and Bodies of Revolution," Grumman Rept. 390-71-1, 1971, Grumman Corp., Bethpage, N.Y.

[12] Murman, E. M., "Analysis of Embedded Shock Waves Calculated by Relaxation Methods," *AIAA Journal*, Vol. 12, May 1974, pp. 626–633.

[13] Roache, P. J., "Finite-Difference Methods for the Steady-State Navier-Stokes Equations," Rept. SC-RR-72 0419, 1972, Sandia Labs., Albuquerque, N. Mex.

[14] Widlund, O. B., "On the Use of Fast Methods for Separable Finite-Difference Equations for the Solution of General Elliptic Problems," in *Sparse Matrices and Their Applications*, edited by D. J. Rose and R. A. Willoughby, Plenum Press, New York, 1972, pp. 121–134.

[15] Concus, P. and Golub, G. H., "Use of Fast Direct Methods for the Efficient Numerical Solution of Nonseparable Elliptic Equations," *SIAM Journal on Numerical Analysis*, Vol. 10, Dec. 1973, pp. 1103–1120.

[16] Roache, P. J., *Computational Fluid Dynamics*, Hermosa Publishers, Albuquerque, New Mex., 1972.

[17] Martin, E. D., "A Generalized-Capacity-Matrix Technique for Computing Aerodynamic Flows," *Presented at the Symposium on Application of Computers to Fluid Dynamics Analysis and Design*, Polytechnic Institute of Brooklyn Graduate Center, Farmingdale, New York, 1973; also *Computers and Fluids*, Vol. 2, March 1974, pp. 79–97.

[18] Martin, E. D. and Lomax, H., "Rapid Finite-Difference Computation of Subsonic and Transonic Aerodynamic Flows," AIAA Paper 74-11, Washington, D.C., 1974.

[19] Aitken, A. C., "On Bernoulli's Numerical Solution of Algebraic Equations," *Proceedings of the Royal Society of Edinburgh*, Vol. 46, 1926, pp. 289–305.

[20] Shanks, D., "Non-Linear Transformations of Divergent and Slowly Convergent Sequences," *Journal of Mathematics and Physics*, Vol. 34, April 1955, pp. 1–42.
[21] Bellman, R., *Methods of Nonlinear Analysis*, Vol. 1, Academic Press, New York, 1970.
[22] Henrici, P., *Elements of Numerical Analysis*, Wiley, New York, 1964.
[23] Hafez, M. M. and Cheng, H. K., "On Acceleration of Convergence and Shock-Fitting in Transonic Flow Computations," Memorandum, Dept. of Aerospace Engineering, University of Southern Calif., Los Angeles, 1973.
[24] Steger, J. L. and Lomax, H., "Generalized Relaxation Methods Applied to Problems in Transonic Flow," *Lecture Notes in Physics*, Vol. 8, Springer-Verlag, Berlin, 1971, pp. 193–198.
[25] Cole, J. D., *Perturbation Methods in Applied Mathematics*, Blaisdell, Waltham, Mass., 1968.
[26] Ashley, H. and Landahl, M., *Aerodynamics of Wings and Bodies*, Addison-Wesley, Reading, Mass., 1965.

MAY 1975 AIAA JOURNAL VOL. 13, NO. 5

Subsonic Cascade Flutter with Finite Mean Lift

MASANOBU NAMBA*
Kyushu University, Fukuoka, Japan

This paper gives a method of calculating the unsteady aerodynamic forces and predicting the flutter conditions for unstalled two-dimensional cascade blades operating with finite mean lift force in subsonic flows. In this method the unsteady effect of the oscillatory motion of a pressure dipole of a finite steady strength is represented by the equivalent effect of a stationary pressure quadrupole with a fluctuating strength, and all the disturbance quantities are treated on the basis of linearization. Some numerical results are provided for a cascade of flat plates in translational oscillation at finite mean angle of attack. The effect of the Mach number upon the unsteady aerodynamic forces and the marginal flutter conditions are investigated. The critical reduced frequency for a given angle of attack decreases for compressor cascades, while it increases for turbine cascade with increase in the Mach number. The contribution of the finite time mean part of the lift force to the unsteady component of the lift force is heavily influenced by the Mach number. The possibility of negative aerodynamic damping at the resonance conditions is indicated.

Nomenclature

$\bar{C}_L$ = mean lift coefficient defined by Eq. (32)
$\tilde{C}_L, \tilde{C}_{La}, \tilde{C}_{Lr}$ = unsteady lift coefficient defined by Eq. (33)
c = blade chord
$\bar{K}_p, K_{pa}, K_{pr}$ = kernel functions for disturbance pressure [see Eqs. (5–10) and Appendix A]
$\bar{\mathbf{Ku}}, \mathbf{Ku}_a, \mathbf{Ku}_r$ = kernel functions for disturbance velocity [see Eqs. (21–23)]
$\bar{K}_v, K_{va}, K_{vr}$ = y-components of $\bar{\mathbf{Ku}}$, $\mathbf{Ku}_a$, $\mathbf{Ku}_r$ respectively (see Appendix B)
M_o = Mach number of undisturbed flow
p = disturbance pressure
$\bar{p}$ = mean disturbance pressure
s = pitch/chord ratio
t = dimensionless time scaled with respect to c/U_o
U_o = undisturbed velocity of fluid
$\mathbf{u}$ = disturbance velocity
$\bar{\mathbf{u}}$ = mean disturbance velocity
$\tilde{v}, \tilde{v}_a, \tilde{v}_r$ = y-components of $\tilde{\mathbf{u}}$, $\tilde{\mathbf{u}}_a$, $\tilde{\mathbf{u}}_r$ respectively
x, y = dimensionless coordinates scaled with respect to c (see Fig. 2)
$\bar{z}(x)$ = mean position of the blade camber (see Fig. 2)
$\bar{\alpha}_{-\infty}$ = mean angle of attack (see Fig. 2)
γ = angle of stagger (see Fig. 2)
$\delta(\,)$ = Dirac's delta function
$\Delta\bar{p}_B(x)$ = mean pressure jump across a blade
ε = nondimensional small quantity
$\varepsilon a(x)\, e^{i\lambda t}$ = displacement of the blade scaled with respect to c (see Fig. 2)
$\varepsilon\tilde{p}_a\, e^{i\lambda t}$ = unsteady component of disturbance pressure due to unsteady pressure dipoles
$\varepsilon\tilde{p}_r\, e^{i\lambda t}$ = unsteady component of disturbance pressure due to unsteady pressure quadrupoles
$\varepsilon\Delta\tilde{p}_B(x)\, e^{i\lambda t}$ = unsteady part of pressure jump across a blade
$\varepsilon\Delta\tilde{p}_{Ba}(x)\, e^{i\lambda t}$ = the first component of $\varepsilon\Delta\tilde{p}_B(x)\, e^{i\lambda t}$
$\varepsilon\Delta\tilde{p}_{Br}(x)\, e^{i\lambda t}$ = the second component of $\varepsilon\Delta\tilde{p}_B(x)\, e^{i\lambda t}$
$\varepsilon\tilde{\mathbf{u}}_a\, e^{i\lambda t}$ = unsteady component of disturbance velocity due to unsteady pressure dipoles
$\varepsilon\tilde{\mathbf{u}}_r\, e^{i\lambda t}$ = unsteady component of disturbance velocity due to unsteady pressure quadrupoles
λ = reduced frequency ($= \omega c/U_o$)
σ = interblade phase angle divided by 2π
ρ_o = density of undisturbed fluid
ω = angular frequency of blade oscillation
$\mathscr{R}(\,)$ = real part
$\mathscr{I}(\,)$ = imaginary part

I. Introduction

IN the past 20 years many studies have been done on the vibration of cascade blades, and the theoretical methods of treating the unstalled cascade flutter for two-dimensional incompressible flows are well developed.[1–3] However, modern axial compressors and turbines are designed to operate in high subsonic or transonic flow conditions, and there exists an urgent need to establish a method of predicting the compressibility effect upon the cascade flutter.

In most of the theoretical work done on the vibration of cascade blades in compressible flows, it has been assumed that the mean deflection of the air through a cascade is very small or zero.[4–6] According to the incompressible flow theories, however, the unstalled bending flutter can not occur unless the mean deflection of the air (in other words, the mean lift force on the blades) is large. In order to account for the bending flutter therefore, it is essential to allow for the finite mean lift force.

Any approach to the problem will encounter a great difficulty in mathematical treatments if it strictly takes account of both

Received July 1, 1974; revision received October 25, 1974. This work was partially supported by the Science Research Fund of the Ministry of Education of Japan.
Index categories: Subsonic and Transonic Flow; Nonsteady Aerodynamics.
* Associate Professor, Department of Aeronautical Engineering.